DR SOON-KI PARK (Orcid ID : 0000-0001-6950-9460)

Article type : Original Article

MYB81, a microspore-specific GAMYB transcription factor, promotes pollen mitosis I and cell lineage formation in Arabidopsis.

Sung-Aeong Oh[1], Thuong Nguyen Thi Hoai[1], Hyo-Jin Park[1], Mingmin Zhao[2], David Twell[2], David Honys[3] and Soon-Ki Park[1]✉

[1]School of Applied Biosciences, Kyungpook National University, Daegu 41566, Republic of Korea.
[2]Department of Genetics and Genome Biology, University of Leicester, University Road, Leicester LE1 7RH, UK.
[3]Laboratory of Pollen Biology, Institute of Experimental Botany of the Czech Academy of Sciences, v.v.i., Prague, Czech Republic.

✉**For correspondence:** fax +82 53 958 6880; e-mail psk@knu.ac.kr

Running head: AtMYB81 promotes pollen mitosis I.
Keywords: *Arabidopsis,* MYB81, microspore, pollen mitosis I, transcription factor, vacuole
Total Figures and Tables: 7 Figures (5 supplemental Figures, 7 supplemental Tables)
Total words included for count: 6,385
Words for all sections: Summary, 207; **Introduction**, 806; **Results**, 2,215; **Discussion**, 1,353; **Experimental Procedures**, 859; **Acknowledgements**, 77; References, 1,818; Short legends for supporting information, 125; **Figure legends**, 868; Full legends for supporting information, 393.

SUMMARY

Sexual reproduction in flowering plants relies on the production of haploid gametophytes that consist of germline and supporting cells. During male gametophyte development, the asymmetric mitotic division of an undetermined unicellular microspore segregates these two cell lineages. To explore genetic regulation underlying this process, we screened for pollen cell patterning mutants and isolated the heterozygous *myb81-1* mutant that sheds ~50 % abnormal pollen. Typically, *myb81-1* microspores fail to undergo pollen mitosis I and arrest at polarized stage with a single central vacuole. Although most *myb81-1* microspores degenerate without division, a small fraction divide at later stages and fail to acquire correct cell fates. The *myb81-1* allele is transmitted normally through the female, but rarely through pollen. We show that *myb81-1* phenotypes result from impaired function of the GAMYB transcription factor *MYB81*. The *MYB81* promoter shows microspore-specific activity and a MYB81-RFP fusion protein is only expressed in a narrow window prior to pollen mitosis I. Ectopic expression of *MYB81* driven by various promoters can severely impair vegetative or reproductive development, reflecting the strict microspore-specific control of *MYB81*. Our data demonstrate that MYB81 has a key role in the developmental progression of microspores, enabling formation of the two male cell lineages that are essential for sexual reproduction in Arabidopsis.

INTRODUCTION

The life cycle of flowering plants depends upon alternation of dominant diploid and highly reduced haploid gametophyte phases. It is the gametophytes that produce the gametes needed for double fertilization and plant fertility. In the carpel of the flower, a common developmental pattern involves meiosis followed by three rounds of mitosis leading to the differentiation of a seven-celled female gametophyte (Drews and Koltunow, 2011). On the other hand, a two or three-celled male gametophyte develops within the anther locule of the stamen (McCormick, 1993; Berger and Twell, 2011). Only three consecutive cell divisions are required to establish the necessary genetic and cellular capacity of the male gametophyte to achieve double fertilization. Meiosis in diploid pollen mother cells produces tetrads of haploid microspores. After release from the tetrad, microspores grow in size and accumulate a tough exine wall. In parallel, vacuoles distributed throughout the microspore cytoplasm coalesce to form a single central vacuole, while the nucleus migrates to the germ cell pole. The polarized microspore undergoes a highly asymmetric division, termed pollen mitosis I (PMI), segregating two distinct daughter cell lineages. The larger vegetative cell differentiates to enable its role in sperm cell delivery to the ovule, while the generative cell divides at pollen mitosis II (PMII) to form two sperm cells. After pollination, the pollen tube is guided to the embryo sac into which the sperm cells are discharged.

Pollen development is excellent system in which to study the control of cellular development, yet only a handful of genes are known to play a role in pollen cell patterning (McCormick, 1993; Twell, 2011). The

important role of microspore division asymmetry in the differentiation of the two pollen cell lineages is well established (Twell *et al.*, 1998). For example, when tobacco microspores are cultured in the presence of colchicine, cells may divide equally or remain undivided (Eady *et al.*, 1995). In both cases microspores adopt vegetative cell fate as the default state and are able to produce a pollen tube. Equally divided or single-celled pollen grains formed in different Arabidopsis mutants also express vegetative cell fate markers as default. These include those which disturb microspore polarity and pollen cytokinesis, such as *gemini pollen 1* (*gem1*) (Park *et al.*, 1998) and combinations affecting the cell cycle regulators CDKA;1, FBL17 and E2F (Glöckle *et al.*, 2018) or helix-loop-helix transcription factors (Zhang *et al.*, 2017).

The development of undetermined microspores can be dissected into three stages – (1) cell polarization, involving nuclear migration to the germ cell pole, (2) oriented nuclear division along a predefined axis, (3) spatially guided cytokinesis to isolate the two distinct daughter cell lineages (Twell *et al.*, 1998, Oh *et al.*, 2011). All three steps are mis-regulated in mutants affecting microtubule dynamics. Cell polarization at stage (1) is disturbed by *gem1* alleles of *MOR1* (Whittington et al., 2001), which encodes microtubule-associated protein MAP215 family (Twell *et al.*, 2002). Some *gem1* microspores divide after incomplete polarization to produce equally-sized daughter cells that express vegetative cell fate (Park *et al.*, 1998; Oh *et al.*, 2010). Other proteins with microtubule-based functions that affect spindle stability or orientation at PMI include γ-tubulins TUBG1 and TUBG2 (Pastuglia *et al.*, 2006), the γ-tubulin targeting factor NEDD1 (Zeng *et al.*, 2009) and members of the AUGMIN complex (Ho *et al.*, 2011; Hotta *et al.*, 2012; Oh *et al.*, 2016). Regarding oriented nuclear division during stage (2), microspores in *sidecar pollen* (*scp*) mutants show delayed entry into PMI with disturbed spindle orientation, which can result in 'four-celled' pollen grains with an extra vegetative cell (Chen *et al.*, 1997; Oh *et al.*, 2010). *SCP* encodes a microspore-specific member of the Lateral Organ Boundaries Domain (LBD) protein family that is proposed to module transcriptional networks determining the timing and orientation of division at PMI (Chen *et al.*, 1997; Oh *et al.*, 2010). Stage (3) is blocked in cytokinesis-defective *two-in-one* (*tio*) mutants, leaving two nuclei in the same cytoplasm without cell lineage segregation. Similar defects are documented for mutant alleles of two pairs of kinesins which show functional redundancy, KINESIN-12A and KINESIN-12B (Lee *et al.*, 2007) and HINKEL and TETRASPORE (Oh *et al.*, 2008). Overall, these studies provide a genetic framework underlying asymmetric PMI, but further analysis of components which act prior to PMI are needed to fully dissect the process.

In this study we present the genetic and phenotypic analysis of the *myb81-1* mutant in which microspores arrest after cell polarization at the threshold of PMI. We identify the lesion as an impaired function allele of the GAMYB transcription factor MYB81. We show that the activity of the *MYB81* promoter and the expression of a MYB81 fusion protein are both restricted to microspores. Our data show that MYB81 is

required for the advancement of microspores into PMI and therefore has a key role in the formation of the two cell lineages essential for pollen development in Arabidopsis.

RESULTS

Isolation and genetic analyses of *myb81-1* mutant

To isolate genes involved in pollen developmental patterning, we screened an activation-tagging pool for plants that shed pollen with altered numbers of nuclei (see Experimental procedures). This led to the isolation of a mutant which produced ~50% of pollen with abnormal phenotypes including aborted pollen and pollen with various numbers of nuclei. We showed that the mutant was heterozygous for a lesion in the GAMYB transcription factor MYB81 and the mutant allele was termed *myb81-1* (see below for details). The *myb81-1* mutant was backcrossed three times with L*er*-0 and the resulting progeny were used for further analyses.

When mature pollen was examined from wild type, 96.7% (n=4,207) were typical tricellular pollen (Figure 1a, Table S1), while the remaining 3.3% comprised mainly degenerated pollen (3.2%, Figure 1b,c) and occasionally pollen containing one or two nuclei (0.1%). In contrast, heterozygous and homozygous *myb81-1* mutants produced 48.5% (n=7,186) and 0% (n=1,191) normal tricellular pollen respectively (Table S1, Figure 1a). Degenerated pollen (Figure 1b,c) was the most common class of abnormal pollen in *myb81-1* mutants, comprising 45.2% and 99.5% in heterozygous and homozygous mutants respectively, while other abnormal types with altered numbers of nuclei (Figure 1d-l) were 6.2% and 0.5% respectively. Interestingly, some pollen grains were either ruptured with vegetative cytoplasm exposed (Figure 1e,h,k), or appeared highly vacuolated (Figure 1f,i,l).

The growth and development of *myb81-1* mutants was similar to that of wild type plants, except that carpels in *myb81-1* homozygotes did not produce elongated siliques (Figure S1). We observed complete ovule abortion in the unelongated carpels of homozygous *myb81-1* mutants (100%, n>1,000), compared to the low levels in unelongated siliques of wild type (7.7%, n=1,616) and heterozygous *myb81-1* (11.3%, n=1,048) plants. To clarify whether ovule abortion was due to abnormal female gametogenesis, we fertilized pistils of homozygous *myb81-1* plants with wild type pollen. The resulting siliques showed ~6.8% ovule abortion (n=355), which is equivalent to that in wild type and heterozygous *myb81-1* plants (Figure S1). These data indicate that *myb81-1* has no discernible effect on the female gametophyte.

The pollen-specific defects observed in *myb81-1* mutants were reflected in the results of our genetic transmission analysis, which involved reciprocal crosses between wild type and heterozygous *myb81-1* mutants. These data revealed a frequency of only 0.7 % for transmission of *myb81-1* through the male gametes (n=300) compared with the wild type allele, whereas transmission of *myb81-1* through the female gametes was not significantly affected (Table S2). Based on the frequency of mutant plants arising from

each reciprocal cross, ~47.2 % heterozygous and 0.3 % homozygous mutants were expected among the self-progeny of heterozygotes. These are similar to the observed frequencies of heterozygous (52.0 %) and homozygous (1.0 %) plants (n=1,200). These data confirm that *myb81-1* defects are restricted to the male gametophyte.

***myb81-1* microspores fail to enter PMI.**

To determine the origin of abnormal pollen phenotypes in *myb81-1* mutants, we examined DAPI-stained spores from staged bud samples in wild type and *myb81-1* mutant plants (Figure 2 and Table S3). In wild type bud samples, typical landmark events were observed (Figure 2a-h,t). When released from the tetrad, individual microspores accumulate exine and become polarized, with a single central vacuole and an eccentric nucleus (Figure 2a-d). Asymmetric division at PMI gives rise to bicellular pollen with a larger vegetative cell and a smaller generative cell separated by a curved generative cell wall (Figure 2e). The internalized generative cell (Figure 2f) elongates (Figure 2g) before dividing to produce tricellular pollen containing two sperm cells (Figure 2h).

Developing microspores of *myb81-1* heterozygotes and wild type plants were indistinguishable until the polarized stage (Figure 2i-l). In *myb81-1* heterozygotes after PMI, when approximately half of microspores reached the bicellular stage (Figure 2e), the other half remained undivided with an eccentric nucleus and a single central vacuole (Figure 2m). By examining later stages it became evident that *myb81-1* microspores arrest at polarized microspore stage and fail to undergo PMI. Typically, *myb81-1* microspores degenerate without division and nuclei are less discernible (Figure 2m-p,t). Occasionally *myb81-1* microspores divide later, resulting in larger pollen with two nuclei and abundant organellar DNA (compare Figure 2q-s and Figure 2e). Nearly all abnormal pollen grains belong to the degenerating pollen class (AbDEG) and microspores dividing at later stages were rare (AbEBC, 2.7 %~4.2 % in Table S3). Further, all abnormal pollen phenotypes observed in heterozygous *myb81-1* plants occurred at higher frequencies in homozygous mutants (Figure S2 and Table S3). These data show that the advancement of microspores into PMI is blocked or delayed in *myb81-1* mutants.

Vacuole dynamics associated with PMI is impaired in *myb81-1*.

Our observations of developing pollen suggested that the *myb81-1* microspores not only fail to enter mitosis, but also display abnormal vacuole dynamics (Figure 2). To better visualize vacuole organization in wild type and *myb81-1*mutant plants, developing microspores were examined after staining with the vacuole-selective dye Neutral Red (Whitley et al, 2009; Figure 3a-f). Vacuoles were also visualized with the tonoplast marker, VHA-A:mRFP1, encoding vacuolar H^+ ATPase subunit A (VHA-A) fused to mRFP1. Consistent with previous observations of vacuolar dynamics in the wild type (Dettner *et al.*, 2005), small distributed vacuoles in early microspores (Figure 3g) merge to form a single large vacuole (Figure 3a,h),

which then divides into smaller ones soon after PMI (Figure 3b,c,i,j). From tricellular stage onwards, even smaller vacuoles are densely packed around a central region of cytoplasm (Figure 3d,k). In contrast, the large central vacuole formed at polarized microspore stage is persistent in *myb81-1* and continues to expand, occupying most of cytoplasmic space (Figure 3e,f,l). Thus, the dynamic changes in vacuolar fission closely linked to PMI are clearly disturbed in *myb81-1* microspores.

***myb81-1* pollen fails to establish two cell lineages essential for sexual reproduction.**

To monitor cell differentiation in *myb81-1* pollen, vegetative cell or germline fate markers were introduced into wild type and mutant plants. The late anther tomato 52 (*LAT52*) promoter (Twell, 1992) directs histone H2B-fluorescent protein expression to the vegetative cell (Figure 4a), while the promoter of the male gamete–specific histone H3.3 variant *HTR10* (also known as MGH3; Okada *et al.*, 2005) marks sperm cell nuclei (Figure 4a). Consistent with the notion that vegetative cell fate is inherited as default when microspore nuclear division fails (Eady et al., 1996; Park et al., 1998; Glöckle *et al.*, 2018), almost all single nucleate *myb81-1* pollen, only expressed the LAT52-H2B-GFP marker (Figure 4b), In rare cases, comprising less than 1 % of *myb81-1* pollen, we observed the unexpected expression of cell fate markers (Figure 4c-e). These included single-nucleate cells expressing both cell fate markers (Figure 4c) and other divided pollen types with mixed cell fate (Figure 4d,e). Collectively, these data show that *myb81-1* mutant microspores fail to establish a separate differentiated male germline. This most likely accounts for the complete sterility observed in homozygous *myb81-1* plants.

A mutation in *MYB81* is responsible for the mutant pollen phenotypes.

The locus responsible *myb81-1* mutant phenotypes was identified by map-based cloning (see Experimental procedures). The *myb81-1* locus was narrowed down to a ~37-Kb region between the markers 26940 and 27030 (Figure 5a). We sequenced coding regions for all 11 candidate genes in the region and detected a 6 bp deletion in the R2 domain of At2g26960, which encodes the R2R3 MYB domain transcription factor MYB81 (Figure 5a, Table S5). The deleted 6 bp sequence, TACGTT, at nucleotide positions 106-111, corresponds to codons for tyrosine (Y36) and valine (V37). When we sequenced the *MYB81* cDNA from wild type Col-0 plants, we found that *MYB81* comprises 3 exons and 2 introns, instead of 2 exons and 1 intron annotated at The Arabidopsis Information Resource (www.arabidopsis.org). By sequencing further *MYB81* cDNA samples from wild type L*er-0* and *myb81-1* mutant plants, we confirmed that *MYB81* encodes a protein of 405 aa instead of 427 aa (Figure 5a, Figure S3). As T-DNA insertional mutations were not available at the *MYB81* locus we performed complementation analysis by transforming heterozygous *myb81-1* mutants with a Hyg^R vector (proMYB81-MYB81) containing the *MYB81* promoter region and the wild-type *MYB81* cDNA. T1 Hyg^R plants were genotyped into 52 wild type and 49 heterozygous and 11 homozygous *myb81-1* mutants by PCR analysis using two sets of allele-specific primers (Table S4).

Phenotypic analysis showed that the vector significantly decreased the frequency of abnormal pollen phenotypes in heterozygous and homozygous *myb81-1* mutants (Figure 5b) and rendered completely sterile homozygous *myb81-1* plants fertile with elongated siliques (Figure S4a-f). When we germinated T2 seeds from 3 heterozygous and 1 homozygous *myb81-1* mutants that showed approximately 25% and 50% abnormal pollen grains respectively, their segregation ratio on Hyg-supplemented media was close to 3 resistant:1 sensitive (Figure S4g). In addition, when 10 Hyg^R T2 seedlings per line were grown, homozygous *myb81-1* plants were detected at highly increased frequencies and all produced fully elongated siliques (Figure S4h). Taken together, these results confirm that *MYB81* is responsible for the *myb81-1* mutant pollen phenotypes.

MYB81 expression is restricted to unicellular microspores.

We examined public transcriptomic data for *MYB81* and found that signals are generally low or absent with prominent peaks only in microspores and bicellular pollen grains (Table S6). Semi-quantitative RT-PCR analysis revealed that *MYB81* transcripts are only detected in young flower buds among the sporophytic samples examined (Figure 5c). Transcripts were not detected in mature pollen, but maximum signals were present in isolated spore fractions enriched for microspores and bicellular pollen (Figure 5d).

To further explore *MYB81* expression, we generated transgenic lines containing promoter fusion GUS reporter constructs with (proMYB81-MDB-GUS) or without (proMYB81-GUS) a region encoding the Arabidopsis CYCLIN B1;1 (*CYCB1;1*) mitotic destruction box (MDB). The CYCB1;1 MDB was used to distinguish persistent GUS protein from active transcription/translation. When 50 T1 plants for each construct were examined, 42 proMYB81-GUS and 45 proMYB81-MDB-GUS plants showed GUS-staining in young buds. The use of the MDB restricted GUS detection to even younger buds, which are likely to contain developing microspores (Figure 5e,f). On the other hand, GUS-staining was not detected in seedlings of 20 T2 proMYB81-GUS lines examined (Figure 5g). These results are in accord with the male-specific defects of *myb81-1,* which first appear at early stages of pollen development.

We further investigated the temporal and spatial expression of MYB81 using transgenic lines expressing a MYB81-mRFP1 fusion protein under control of the MYB81 promoter. RFP signals were not detected in mature pollen from 50 T1 plants. However, when microspores and developing pollen from young buds were examined, 36 out of 40 lines displayed RFP signals that were confined to nuclei. To precisely monitor the temporal and spatial expression of MYB81, we examined pollen from serially staged bud samples from multiple lines at T1 and T2 generations. The results showed that MYB81-mRFP1 is not detectable in early microspores immediately after their release from tetrads (Figure 5h). Expression is first visible in the centrally positioned microspore nucleus and remains detectable until the cell becomes polarized (Figure 5i-k). After PMI, RFP signals were no longer detected (Figure 5l-o). Interestingly, in transgenic lines containing a vector in which *MYB81* was replaced with the coding region of histone H2B (proMYB81-

H2B-mRFP1), RFP signals were first detected in microspores but persisted in mature pollen (Figure 5p-w). These results show that *MYB81* expression is specific to microspores and that the narrow window of *MYB81* protein expression is subject to further post-transcriptional controls.

Ectopic expression of *MYB81* severely hinders normal plant development.

To investigate whether alteration of the microspore-specific expression of MYB81 would impact on other stages of development, we generated transgenic lines directing MYB81 to the pollen vegetative cell (proLAT52-MYB81-GFP) or to male germline cells (proDUO1-MYB81-mRFP1). Unlike the proLAT52-H2B-GFP control lines that marked the vegetative nucleus in mature pollen (Figure 6a), proLAT52-MYB81-GFP lines (n=50) dehisced degenerating and dead pollen without GFP signals (Figure 6b,f). In younger buds of proLAT52-MYB81-GFP lines, GFP signal was observed in the vegetative nucleus of developing pollen (Figure 6c). Among segregating T2 progeny, those with a normal pollen phenotype did not give GFP signals in pollen, but those with degenerating pollen gave strong GFP signals only in developing pollen. Thus, we conclude that ectopic MYB81 expression in the vegetative cell leads to cellular degeneration.

On the other hand, when pollen was examined from open flowers of proDUO1-MYB81-mRFP1 lines (n=50), high levels of bicellular pollen grains were present (Figure 6e,g). Among T2 progeny two groups could be distinguished, one with normal tricellular pollen, negative for RFP in sperm (Figure 6d), and the other with significant levels of bicellular pollen, positive for germline-specific RFP (Figure 6e). Thus, ectopic MYB81 expression in the male germline is associated with failure of cell division.

When constitutive overexpression constructs (proUBQ14-MYB81 and pro35S-MYB81-dHA) were introduced into wild type plants, we were unable to rescue transgenic lines despite repeated efforts. However, constructs expressing the *myb81-1* cDNA generated T1 lines at typical frequencies and all 50 T1 plants were phenotypically normal. We also assessed the localization of wild type MYB81 and mutant MYB81-1 proteins in vegetative tissues. Since a constitutive promoter could not be used for wild type MYB81, we produced plants with an estradiol-inducible construct (proXVE-MYB81-mRFP1), while pro35S-myb81-1-mRFP1 was used for to express the mutant MYB81-1 protein. The estradiol-induced MYB81:mRFP1 (Figure 6i) and the constitutively-expressed MYB81-1:mRFP1 (Figure 6j) proteins both localised to nuclei in the roots of seedlings. Taken together, our results indicate that constitutive overexpression of MYB81 is likely to cause embryo lethality.

DISCUSSION

We have identified a male gametophyte-specific mutant in which pollen development arrests at the polarized microspore stage. Through map-based cloning, complementation and expression analyses, we show that a mutant allele (*myb81-1)* of the *MYB81* locus is responsible. Our data demonstrate that MYB81

is a microspore-specific member of the GAMYB transcription factor family required for the advancement of polarized microspores into PMI. MYB81 enables the asymmetric cell division at PMI that establishes the two cell lineages required for pollen patterning and plant fertility.

MYB81 is a non-redundant GAMYB family member.

MYB81 belongs to subgroup 18 of R2R3 MYB transcription factor proteins (Du *et al.,* 2015), also known as the GAMYB family (Figure 7b,c). Phylogenetic analysis has revealed that the R2R3 S18 GAMYB family is sister to the DUO1 R2R3 MYB family (Du *et al.,* 2015; Higo *et al.*, 2018). The GAMYB and DUO1 R2R3 MYB family are clearly separated in moss and liverworts, with DUO1 directing male germline development and the GAMYB clade specializing male reproductive roles in angiosperms (Higo *et al.*, 2018; Hackenberg and Twell, 2019).

The first identified member of the GAMYB family, *HvGAMYB,* is involved in gibberellin (GA)-regulated gene expression in barley aleurone (Gubler, *et al.*, 1995). In Arabidopsis, the family comprises seven members, *MYB33*, *MYB65*, *MYB81*, *MYB97*, *MYB101*, *MYB104* and *MYB120* (Jiang, *et al.*, 2004; Dubos, *et al.*, 2010). Apart from *MYB81* and *MYB104*, whose functions are yet to be reported, the remaining five GAMYB family members are all involved in different aspects of male reproduction (Millar and Gubler, 2005; Allen *et al.*, 2017; Leydon *et al.*, 2013; Liang *et al.,* 2013).

MYB33 and *MYB65* are close paralogs with critical but redundant roles in anther development (Millar and Gubler, 2005). Similarly, *MYB97*, *MYB101*, and *MYB120* form a distinct clade (Figure 7c) with functionally redundant roles in pollen tube differentiation steps leading to sperm cell release (Leydon *et al.*, 2013; Liang *et al.*, 2013). Although *MYB81* (At2g26960) and *MYB104* (At2g26950) form a paralogous pair, there is no indication of redundancy between them. In fact, based on sequence divergence in important regions of the gene, including the MYB domain, we suggest that *MYB104* may be drifting towards degeneration following its earlier duplication within *Brassicaceae* (Figure 7b,c). Further, there is no *AtMYB104* homolog in the closely related *A. lyrata*, while the homolog in *A. halleri* shows a high rate of mutation within the MYB domain, suggesting relaxation of selection pressure. In the genus *Capsella*, both *C. rubella* and *C. grandiflora* also contain a single *AtMYB81*/*AtMYB104* homolog (Figure 7c).

The expression profiles of all seven Arabidopsis GAMYB family members were compared based on normalized ATH1 microarray data from vegetative and male reproductive tissues, including isolated stages of developing pollen (Table S7). *MYB33* and *MYB65* transcripts are co-expressed in the majority of samples including microspore, bicellular and tricellular pollen stages, although *MYB65* has higher signal values. Transcripts of the *MYB97*, *MYB101* and *MYB120* triad do not have reliable signal values in microspores and all show maximum expression signals in mature pollen and during pollen tube germination (Leydon *et al.*, 2011; Liang *et al.*, 2013). While *MYB81* transcripts are detected in microspore

and bicellular pollen at similar levels, *MYB104* transcripts are considered to be absent in male reproductive and vegetative samples. The distinct early and male-specific profile of *AtMYB81* is consistent with its functional role in microspores and with the failure of homozygous *myb81-1* mutants to produce functional pollen.

MYB81 is required for PMI and cell lineage formation.

Our data show that the expression of MYB81 is restricted to microspores and that impaired function of *MYB81* blocks microspore division. The *myb81-1* mutant allele results in a two-amino acids ($Y_{36}V_{37}$) deletion at the C-terminal end of the first α-helix in the R2 MYB domain of MYB81 (Figure 7a,b). These residues are invariant among Arabidopsis GAMYB family members (Figure 7b) and numerous homologues in other plant species (Figure S5). These changes are likely to affect stability of the hydrophobic core of the MYB domain, which is critical for target sequence recognition and binding (Saikumar *et al.*, 1990; Borg *et al.*, 2011), thereby rendering MYB81-1 loss-of-function. These data indicate that MYB81 may be a positive regulator, but the molecular mechanism by which MYB81 promotes the advancement of microspores into mitosis remains an open question.

One possibility is that MYB81 may directly regulate the expression of proteins involved in cell cycle progression. The cellular patterning and differentiation of pollen requires differential control of the cell cycle in vegetative and generative cells. In Arabidopsis, mutations in several different classes of genes can result in the failure of generative cell division, leading to the formation of bicellular pollen grains in mature anthers. The core cell cycle machinery, such as the A-type cyclin-dependent kinase (CDK) CDKA;1 may be affected as in *cdka;1* mutants, which show retarded S-phase, with only some generative cells able to divide during pollen tube growth (Aw *et al.*, 2010; Iwakawa *et al.*, 2006; Nowack *et al.*, 2005). Regarding progression through G2/M phase transition, the role of DUO1 is well established (Rotman *et al.*, 2005; Brownfield *et al.*, 2009; Borg *et al.*, 2011; Twell, 2011). Mutant generative cells in *duo1* pollen grains complete S-phase, but fail to enter mitosis in part due to reduced accumulation of the mitotic cyclin, CYCB1;1 (Brownfield *et al.*, 2009; Durbarry *et al.* 2005). DUO1 integrates this role with the control of a network of genes required for sperm cell differentiation (Borg *et al.*, 2011; Brownfield *et al.*, 2009). Whether MYB81 regulates mitotic cyclins or acts upon G1/S phase components including those of the CDKA1-RBR-E2F pathway (Kim *et al*., 2008; Chen *et al*., 2009; Zhao *et al*., 2012) remains to be investigated. Further candidates could include canonical E2Fs, as recent work has shown that microspores in triple *e2fabc* mutants degenerate, indicating their requirement for G1/S phase transition (Yao *et al.*, 2018).

It is also possible that MYB81 influences cell cycle progression at PMI indirectly. We observed that microspores of *myb81-1* mutants failed to undergo fission after the failure of PMI (Figures 1-3). The vacuole fulfills numerous essential functions related to metabolism, growth and development (Ruthardt *et*

al., 2005). Plant cells sustain their size and shape with turgor pressures generated from the large central vacuole (Geitmann and Ortega, 2009; Hamant and Traas, 2010; Robinson *et al.*, 2013). Vacuoles also serve as a repository for toxic compounds which may damage sensitive biological processes in the cytoplasm. This implies that vacuolar reorganization should be closely coordinated with other cellular processes to avoid catastrophic events. Vacuoles undergo orchestrated fusion and fission events during the transition of microspores to pollen grains (Yamamoto *et al.*, 2003). These changes may allow the microspore to rebuild its cytoplasm by dismantling organelles inherited from diploid cells (Pacini *et al.*, 2011). This in turn may allow the different subcellular environments to be established which are thought to be necessary for asymmetric division and the cell differentiation events that follow (Twell *et al.*, 1998). Some gametophytic genes are known to have important roles in microspore vacuolar dynamics. In *vacuoleless gametophytes* (*vlg*) mutants which fail to express the DC1 domain protein VLG, microspores fail to undergo vacuolar fusion, nuclear migration and PMI (D'lppólito *et al.*, 2017). In *scp* mutants, which affect the expression of the LBD/ASL family protein LBD27/ASL29, microspore division is delayed and the central vacuole fails to undergo fission (Oh *et al.*, 2010). However, it is unclear whether the persistent central vacuole in *scp* microspores is the cause or consequence of the delayed division. In a further example that is linked to phosphatidylinositol 3,5-bisphosphate [$PI(3,5)P_2$] production, mutation of *VAC14*, hinders vacuolar fission in microspores and division at PMI leading to pollen abortion (Zhang *et al.*, 2018). These studies emphasize an important link between the genetic control of vacuolar reorganization and successful transition to PMI. A plausible scenario is that MYB81 regulates genes involved in microspore vacuolar dynamics so that loss of function perturbs timely vacuole fission, leading to microspore degeneration and blocking entry into PMI. Further studies to identify MYB81 target genes will help to uncover the regulatory network underlying this key developmental transition and essential step in patterning the male gametophyte of flowering plants.

EXPERIMENTAL PROCEDURES

Plant material and growth

The *Arabidopsis thaliana* accessions Columbia-0 (Col-0) and Landsberg *erecta*-0 (L*er*-0) were grown on mixed soil (3 compost: 1 vermiculite) in a controlled growth room under a long-day light regime (16-h light/8-h darkness) at 22 °C. A mutant population used for morphological screening was generated by floral dipping (Clough and Bent, 1998) using L*er*-0 wild type plants with an *Agrobacterium* GV3101 strain harboring the activation tagging vector pSKI015 (Weigel *et al.*, 2000). Although the *myb81-1* mutant line was initially isolated from a T1 population after Basta selection, a co-segregation test between a Basta resistance and the *myb81-1* phenotypes at T2 progeny showed that the *myb81-1* is not associated with a T-DNA insertion. The heterozygous *myb81-1* mutant was backcrossed with L*er*-0 three times to eliminate

unrelated T-DNA insertions and the resulting progenies were used in further analyses.

Genetic analysis and positional cloning of *myb81-1*

The genetic transmission of *myb81-1* was determined by scoring the number of wild type and *myb81-1* plants in F1 progenies arising from reciprocal crosses between wild type (L*er-0*) and heterozygous *myb81-1* plants. For positional cloning, heterozygous *myb81-1* mutant plants (L*er-0*) were fertilized with wild-type Col-0 pollen. F_1 plants were self-fertilized and F2 seeds used to grow mapping populations. Genomic DNA was extracted from 2,908 individual F2 plants using a modified cetyl trimethyl ammonium bromide (CTAB) method as previously described (Oh *et al.*, 2010) and analyzed using PCR-based markers listed in Table S4.

Microscopy

To visualize nuclear composition, mature pollen grains were stained with DAPI solution as described previously (Oh *et al.*, 2010) and viewed by wide-field UV epifluorescence microscopy or confocal laser scanning microscopy (CLSM). Pollen ontogeny analysis was performed using prefixed inflorescences following a procedure described previously (Oh *et al.*, 2010). Fluorescence images were captured using a Nikon Eclipse 80i microscope (Nikon, http://www.microscopyu.com) with the ProgRes MFcool camera set up (Jenoptik, http://www.jenoptik.com). CLSM images were captured using an inverted microscope (C2+, Nikon, Japan) with lasers (excitations at 405nm, 488nm, and 561nm) controlled by NIS-Elements software (Nikon). Inflorescences and seedlings incubated for GUS assays were decolorized in 70% ethanol and bright field images were captured under a stereomicroscope (Nikon) with the ProgRes C3 color camera set up (Jenoptik, http://www.jenoptik.com).

Sequence alignments and phylogenetic analysis

All sequences were collected from Phytozome v12.0 (https://phytozome.jgi.doe.gov). Default parameters were used to align protein sequences with ClustalW (Higgins and Sharp, 1988). Phylogenetic trees were constructed using MEGA 7.0 (Kumar et al., 2016). The maximum likelihood tree was constructed from protein coding nucleotide sequences, using the TN93 model (Tamura and Nei, 1993) and the default bootstrap number of 1000.

Gene expression analysis

Gene expression profiles for *MYB81* were examined by RT-PCR and pMYB81-GUS reporter analyses. For RT-PCR, total RNAs were extracted from sporophytic tissues and isolated male gametophytic cells using the RNeasy Plant Mini kit (Qiagen, Germany). Sporophytic samples included roots, seedlings, rosette leaves, stems, closed bud clusters and open flowers. For male gametophyte samples, fractions enriched for

typical developmental stages were prepared as described by Honys and Twell (2004). First strand cDNA was synthesized using the oligo $d(T)_{18}$ initiated One Step Diastar RT-PCR kit (Solgent, Korea) and further amplified with gene-specific primers for *MYB81* and *HTR8* (At5g10980) using eTaq polymerase (Solgent, Korea). For proMYB81-GUS reporter lines, GUS assays were carried out using inflorescences and seedlings as described (Oh *et al.*, 2010).

Vector construction and generation of transgenic plants

To generate the proMYB81-MYB81 complementation construct, a 1,628-bp genomic fragment immediately upstream of the start codon was amplified with primers tagged with AscI and NotI sites. Full-length *MYB81* cDNA with the stop codon was amplified with primers tagged with NotI and SpeI sites respectively. Both fragments were subcloned into a modified pBlueScript-based vector containing AscI, NotI, and SpeI (Oh *et al.*, 2016). To generate the proMYB81-GUS reporter, the proMYB81 fragment was introduced between AscI and NotI sites in front of the GUS coding region, positioned between NotI and SpeI in an intermediate vector (Oh *et al.*, 2016). The proMYB81-MYB81-mRFP1 construct was built by inserting the full-length MYB81 cDNA without its stop codon downstream of the MYB81 promoter between NotI and SpeI sites. Then, the mRFP1 was subcloned between SpeI and PacI sites in an intermediate vector (Oh *et al.*, 2016). To build proLAT52-MYB81-mRFP1 and proMGH3-MYB81-mRFP1, PCR-amplified proLAT52 and proMGH3 fragments were subcloned into proMYB81-MYB81-mRFP1 by replacing the MYB81 promoter. To generate the constitutive overexpression constructs proUBQ14-MYB81 and pro35S-MYB81, the MYB81 promoter in a proMYB81-MYB81 intermediate vector was replaced with the UBQ14 or CaMV 35S promoter fragments between AscI and NotI sites respectively The proUBQ14-myb81 and pro35S-myb81 vectors to overexpress *myb81* mutant protein used the same restriction sites. All resulting expression cassettes in the pBlueScript-based intermediate vectors were transferred to binary vectors, pER8 or pER10 (Zuo *et al.*, 2000). All primers used for vector construction are listed in supplemental Table S4.

All binary constructs were transformed into *Agrobacterium* strain GV3101 used to transform Arabidopsis plants by a floral dipping (Clough and Bent, 1998). Harvested seeds were surface-sterilized and plated on Murashige & Skoog (MS) media supplemented with 0.6% phytoagar and appropriate antibiotics. Kanamycin, hygromycin and cefotaxime were used at a final concentration of 50 mg/L, 20 mg/L, and 200 mg/L respectively.

ACKNOWLEDGMENTS

This work was supported by a grant from the Next-Generation BioGreen 21 program to S.K.P (no. PJ01369001), Rural Development Administration in the Republic of Korea. D.T. and M.Z. acknowledge support from the Biotechnology and Biological Research Council ERA-CAPS EVOREPRO project (Grant

reference BB/N005090). D.H. was supported from European Regional Development Fund-Project "Centre for Experimental Plant Biology" (No. CZ.02.1.01/0.0/0.0/16_019/0000738). The correctly annotated *MYB81* genomic and cDNA sequences can be found under the accession numbers MN199036 and MN199037 respectively.

CONFLICT OF INTEREST

The authors declare no conflicts of interest.

AUTHORS' CONTRIBUTIONS

SKP, SAO, and DT conceived the research and designed experiments; SAO, TNTH, and HJP performed experiments involved in *myb81-1* mutant characterization, map-based cloning of *MYB81* gene, and various transgenic analysis; MZ and DT performed MYB81 structure and phylogenetic analysis; MZ, DT and DH analyzed transcriptomic datasets for the GAMYB family members; SKP, SAO, and D.T wrote the manuscript with contributions from all authors; SKP and DT supervised the research.

DATA AVAILABILITY STATEMENT

All data associated with the figures and tables are included in the manuscript. Availability of data referred to supplementary materials is indicated in the corresponding legends.

SUPPORTING INFORMATION

Additional Supporting information may be found in the online version is this article:

Figure S1. Plant phenotypes in wild-type and *myb81-1* mutant plants.

Figure S2. Pollen development in wild type and homozygous *myb81-1* mutant plants.

Figure S3. Sequence comparisons for the coding region of *MYB81*.

Figure S4. Complementation analysis of *myb81-1* with proMYB81-MYB81.

Figure S5. Multiple sequence alignment of AtMYB81-1 and other GAMYBs.

Table S1. Mature pollen phenotypes in wild-type and *myb81-1* mutants.

Table S2. Genetic transmission of the *myb81-1* allele.

Table S3. Pollen developmental analysis in wild type and *myb81-1* mutant plants.

Table S4. A list of primers used in this study.

Table S5. Details of the 11 candidate genes in the ~37Kb region and their sequencing results.

Table S6. Expression profiles of *MYB81*.

Table S7. Expression profiles for *GAMYB* genes in Arabidopsis.

REFERENCES

Allen, R.S., Li, J., Stahle, M.I., Dubroue, A., Gubler, F. and Millar A.A. (2007) Genetic analysis reveals functional redundancy and the major target genes of the Arabidopsis miR159 family. Proc. *Nat. Acad. Sci. USA,* **104,** 16371-16376.

Berger, F. and Twell, D. (2011) Germline specification and function in plants. *Annu. Rev. plant Biol.,* **62**, 461-484.

Borg, M., Brownfield, L. and Twell, D. (2009) male gametophyte development: a molecular perspective. *J. Exp. Bot.*, **60(5)**, 1465-1478.

Borg, M., Brownfield, L., Khatab, H., Sidorova, A., Lingaya, M and Twell, D. (2011) The R2R3 MYB transcription factor DUO1 activates a male germline-specific regulon essential for sperm cell differentiation in Arabidopsis. *Plant Cell*, **23**, 534-549.

Borg, M. and Twell, D. (2010) Life after meiosis: patterning the angiosperm male gametophyte. *Biochem. Soc. Trans.,* **38**, 577-582.

Brownfield, L., Hafidh, S., Durbarry, A., Khatab, H., Sidorova, A., Doerner, P. and Twell, D. (2009) *Arabidopsis* DUO POLLEN3 is a key regulator of male germline development and embryogenesis. *Plant Cell*, **21**, 1940-1956.

Chen, Y-C.S. and McCormick, S. (1996) *sidecar pollen*, an *Arabidopsis thaliana* male gametophytic mutant with aberrant cell divisions during pollen development. *Development,* **122**, 3243-3253.

Chen, Z., Hafidh, S., Poh, S. H., Twell, D. and Berger, F. (2009) Hyperproliferation caused by loss of Retinoblastoma prevents cell fate establishment during *Arabidopsis* male gametogenesis. *Proc. Nat.l Acad. Sc.i USA* **106**, 7257-7262.

Clough, S.J. and Bent, A.F. (1998) Floral dip: a simplified method for Agrobacterium-mediated transformation of *Arabidopsis thaliana*. *Plant J.,* **16**, 735-743.

Dettmer, J., Schubert, D., Calvo-Weimar, O., Stiefhof, Y.D., Schmidt, R. and Schumacher, K. (2005) Essential role of the V-ATPase in male gametophyte development. *Plant J.,* **41**, 117-124.

D′lppólito, S., Arias, L.A., Casalongué, C.A., Pagnussat, G.C. and Fiol, D.F. (2017) The DC1-domain protein VACUOLESS GAMETOPHYTES is essential for development of female and male gametophytes in Arabidopsis. *Plant J.,* **90**, 261-275.

Drews, G.N. and Koltunow, A.M.G. (2011) The female gametophyte. The Arabidopsis book, e01155. Doi:10.1199/tab.0155.

Du, H., Liang, Z., Zhao, S., Nan, M-G., Phan Tran, L-S., Lu, K., Huang, Y-B and Li, J-N (2015) The evolutionary history of R2R3-MYB proteins across 50 eukaryotes: new insights into subfamily classification and expansion. *Sci. Rep.,* **5**, 11037.

Dubos, C., Stracke, R., Grotewold, E., Weisshaar, B., Martin, C. and Lepiniec, L. (2010) MYB transcription factors in Arabidopsis. *Trends Plant Sci.,* **15**, 573-581.

Geitmann, A. and Ortega, J.K. (2009) Mechanics and modeling of plant cell growth. *Trends plant Sci.,* **14(9)**, 467-478.

Glöckle, B. Urban, W.J., Nagahara, S., Andersen, E.D., Higashiyama, T., Grini, P. E. and Schnittger, A. (2018). Pollen differentiation as well as pollen tube guidance and discharge are independent ofthe presence of gametes. *Development*, **145**, dev152645.

Gubler, F., Kalla, R., Roberts, J.K. and Jacobsen, J.V. (1995) Gibberellin-regulated expression of a myb gene in barley aleurone cells: evidence for myb transactivation of a high-pI alpha-amylase gene promoter, *Plant Cell*, **7**, 1879-1891.

Hackenberg, D. and Twell, D. (2019) The evolution and patterning of male gametophyte development. *Current Topics in Developmental Biology*, **131**, 257-298.

Hammant, O., and Traas, J. (2010) The mechanics behind plant development. *New Phytol.*, **185(2)**, 369-385.

Higo, A., Kawashima, T., Borg, M., Zhao, M., López-Vidriero, I., Sakayama, H., Montgomery, S.A., Sekimoto, H., Hackenberg, D., Shimamura, M. *etal.* (2018) Transcription factor DUO1 generated by neo-functionalization is associated with evolution of sperm differentiation in plants. *Nat. Commun.,* **9**, 5283.

Higgins, D.G. and Sharp, P.M. (1988) CLUSTAL: a package for performing multiple sequence alignment on a microcomputer. *Gene,* **73**, 237-44.

Ho, C.-M., Hotta, T., Kong, Z., Zeng, C., Sun, J., Lee, Y.-R. and Liu, B. (2011) Augmin plays a critical role in organizing the spindle and phragmoplast microtubule arrays in Arabidopsis. *Plant Cell,* **23**, 2606–18.

Honys, D. and Twell, D. (2004) Transcriptome analysis of haploid male gametophyte development in Arabidopsis. *Genome Biol.*, **5**, R85.1-13.

Hotta, T., Kong, Z., Ho, C.-M., Zeng, C., Horio, T., Fong, S., Vuong, T., Lee, Y.-R. and Liu, B. (2012) Characterization of the Arabidopsis augmin complex uncovers its critical function in the assembly of the acentrosomal spindle and phragmoplast microtubule arrays. *Plant Cell,* **24**, 1494–509.

Kim, H.J., Oh, S.A., Brownfield, L., Hong, S.H., Ryu, H., Hwang, L., Twell, D. and Nam, H.G. (2008) Control of plant germline proliferation by SCF(FBL17) degradation of cell cycle inhibitors. *Nature*, **455**, 1134-1137.

Kumar, S., Stecher, G. and Tamura, K. (2016) MEGA7: Molecular Evolutionary Genetics Analysis Version 7.0 for Bigger Datasets. *Mol. Biol. Evol.,* **33,** 1870-4.

Lee, Y.R.J., Li, Y. and Liu, B. (2007) Two Arabidopsis phragmoplast-associated kinesins play a critical role in cytokinesis during male gametogenesis. *Plant Cell*, **19**, 2595-2605.

Leydon, A.R., Beale, K.M., Woroniecka, K., Castner, E., Chen, J., Horgan, C., Palanivelu, R. and Johnson, M.A. (2013) Three MYB transcription factors control pollen tube differentiation required for sperm release. *Curr. Biol.*, **23**, 1209-1214.

Liang, Y., Tan, Z.M., Zhu, L., Niu, Q.K. Zhou, J.J., Li, M., Chen, L.Q., Zhang, X.Q. and Ye, D. (2013) MYB97, MYB101 and MYB120 function as male factors that control pollen tube-synergid interaction in Arabidopsis thaliana fertilization, *PLoS genetics*, **9**, e1003933.

Long, Y.P., Xie, D.J., Zhao, Y.Y., Sho, D.Q. and Yang, W.C. (2018) BICELLULAR POLLEN 1 is a modulator of DNA replication and pollen development in Arabidopsis. *New Phytol.* **222(1)**, 588-603.

McCormick, S. (1993) Male gametophyte development. *Plant Cell,* **5**, 1265-1275.

Millar, A.A. and Gubler, F. (2005) The Arabidopsis GAMYB-like genes, MYB33 and MYB65, are microRNA-regulated genes that redundantly facilitated anther development. *Plant Cell*, **17**, 705-721.

Murray, M.G. and Thompson, W.F. (1980) Rapid isolation of high molecular weight plant DNA. *Nuc. Acids Res.,* **8**, 4321-4325.

Nowack, M.K., Grini, P.E., Jakoby, M.J., Lafos, M., Koncz, C. and Schnittger, A. (2006) A positive signal from the fertilization of the egg cell sets off endosperm proliferation in angiosperm embryogenesis. *Nat. Genet.*, **38**, 63-67.

Oh, S.A., Bourdon, V., Das, M.P, Dickinson, H. and Twell, D. (2008) Arabidopsis kinesins HINKEL and TETRASPORE act redundantly to control cell plate expansion during cytokinesis in the male gametophyte. *Mol. Plant*, **1**,794-799.

Oh, S.A., Das, M.P., Park, S.K., Johnson, J.A. and Twell, D. (2010) The tobacco MAP215/Dis1-family protein TMBP200 is required for the functional organization of microtubule arrays during male germline establishment. *J. Exp. Bot.*, **61(4)**, 969-981.

Oh, S.A., Jeon, J., Park, H.-J., Grini, P.E., Twell, D. and Park S.K. (2016) Analysis of *gemini pollen 3* mutant suggests a broad function of AUGMIN in microtubule organization during sexual reproduction in Arabidopsis. *Plant J.*, **87**, 188-201.

Oh, S.A., Johnson, A., Smertenko, A., Rahman, D., Park, S.K., Hussey, P.J. and Twell, D. (2005) A divergent cellular role for the FUSED kinase family in the plant-specific cytokinetic phragmoplast. *Curr. Biol.*, **15**, 2107-2111.

Oh, S.A., Park, K.S., Twell, D. and Park, S.K. (2010) The *SIDECAR POLLEN* gene encodes a microspore-specific LOB/AS2 domain protein required for the correct timing and orientation of asymmetric cell division. *Plant J.,* **64**, 839-850.

Okada, T., Endo, M., Singh, M.B. and Bhalla, P.L. (2005) Analysis of the histone H3 gene family in Arabidopsis and identification of the male-gamete-specific variant AtMGH3. *Plant J.*, **44**, 557-568.

Pacini, E., Jacquard, C. and Clément, C. (2011) Pollen vacuoles and their significance. *Planta*, **234**, 217-227.

Park, S.K., Howden, R. and Twell, D. (1998) The *Arabidopsis thaliana* gametophytic mutation *gemini pollen1* disrupts microspore polarity, division asymmetry and pollen cell fate. *Development,* **125**, 3789-3799.

Park, S.K., Raman, D., Oh, S.A. and Twell, D. (2004) *Gemini pollen 2*, a male and female gametophytic cytokinesis defective mutation. *Sex. Plant Reprod.* **17**, 63-70.

Pastuglia, M., Azimzadeh, J, Goussot , M., Camilleri, C., Belcram, K., Evrard, J.L. *et al.*. (2006) Gamma-tubulin is essential for microtubule organization and development in Arabidopsis. Plant Cell **18**, 1412-1425.

Qin, Z., Lv, H., Zhu, X., Meng, C., Quan, T., Wang, M., and Xia, G. (2013) Ectopic expression of wheat WRKY transcription factor gene TaWRKY71-1 results in hyponastic leaves in *Arabidopsis thaliana*. *PloS ONE*, **8**: e63033.

Robinson, S., Burlan, A., Couturier, E., Landrein, B., Louveaux, M., Neumann, E.D., Peaucelle, A., Weber, A. and Nakayama, N. (2013) Mechanical control of morphogenesis at the shoot apex. *J. Exp. Bot.*, **64(15)**, 4729-4744.

Rotman, N., Durbarry, A., Wardle, A., Yang, W.C., Chaboud, A., Faure, J.E., Berger, F. and Twell, D. (2005) A novel class of MYB factors controls sperm-cell formation in plants. *Curr. Biol.,* **15**, 244-248.

Ruthardt, N., Gulde, N., Spiegel, H., fischer, R., and Emans, N. (2005) Four-dimensional imaging of transvacuolar strand dynamics in tobacco BY-2 cells. *Protoplasma*, **225,** 205-215.

Saikumar, P., Murali, L.J. and Reddy, E.P. (1990) Role of tryptophan repeats and flanking amino acids in Myb-DNA interactions. *Proc. Natl. Acad. Sci. USA,* **87**, 8452-8456.

Takeda, T., Amano, K., Ohto, M., Nakamura, K., Sato, S., Kato, T., Tabata, S., and Ueguchi, C. (2006) RNA interference of the *Arabidopsis* putative transcription factor *TCP16* gene results in abortion of early pollen development. *Plant Mol. Biol*., **61**, 165-177.

Tamura, K. and Nei, M. (1993) Estimation of the number of nucleotide substitutions in the control region of mitochondrial DNA in humans and chimpanzees. *Mol. Biol. Evol.,* **10,** 512-26.

Twell, D. (1992) Use of a nuclear–targeted β-glucuronidase fusion protein to demonstrate vegetative cell-specific gene expression in developing pollen. *Plant J.*, **2**, 887-892.

Twell, D. (2011) Male gametogenesis and germline specification in flowering plants. *Sex Plant Reprod.,* **24**,149-160.

Twell, D., Park, S.K., Hawkins, T.J., Schubert, D., Schmidt, R., Smertenko, A, *et al.* (2002) MOR1/GEM1 plays an essential role in the plant-specific cytokinetic phragmoplast. *Nat. Cell Biol.,* **4**, 711-714.

Twell, D., Park, S.K. and Lalanne, E. (1998) Asymmetric division and cell-fate determination in developing pollen. *Trends Plant Sci.,* **3(8)**, 305-310.

Whitley, P., Hiz, S. and Doughty, J. (2009) Arabidopsis FAB1/pIKfyve proteins are essential for development of viable pollen. *Plant Physiol.*, **109**, 146-159.

Wiegel, D., Ahn J.H., Blázquez, M.A., Borevitz, J.O., Christensen, S.K., Fankhauser, C., Ferrándiz, C., Kardailsky, I., Mamancharuvil, E.J., Neff, M.M., *et al.* (2000) Activation tagging in Arabidopsis.

Plant Physiol., **122**, 1003-1013.

Yamamoto, Y., Nishimuta, M., Hara-Nishimuta, I. and Noguchi, T. (2003) Behavior of vacuoles during microspore and pollen development in Arabidopsis thaliana. *Plant Cell Physiol.,* **44(11)**, 1192-1201.

Yao, X., Yang, H., Zhu, Y., Xue, J., Wang, T., Song, T., Yang, Z. and Wang, S. (2018) The canonical E2Fs are required for germline development in Arabidopsis. *Front. Plant Sci.,* Doi:10.3389/fpls.2018.00638.

Zeng C.J.T., Lee, Y.R.J, Liu, B. (2009) The WD40 repeat protein NEDD1 function in microtubule organization during cell division in *Arabidopsis thaliana*. *Plant Cell*, **21**, 1129-1240.

Zhang., W.-T., Li E., Guo, Y.-K., Yu, S.-X., Wan, Z.-Y., Ma, T., Li, S., Hirano, T., Sato, M.H. and Zhang, Y. (2018) Arabidopsis *VAC14* is critical for pollen development through mediating vacuolar organization. *Plant Physiol.*, DOI:10.1104/pp.18.00495.

Zhang, J., Huang, Q.P., Zhong, S., Bleckmann, A., Huang, J.Y., Guo, X.Y, Lin, Q, Gu, H.Y., Dong, J., Dresselhaus T., Qu, L.J. (2017) Sperm cells are passive cargo of the pollen tube in plant fertilization. *Nat. Plants*, **3**, 17079.

Zheng, Z., Reichel, M., Deveson, I., Wong, G., Li, J. and Millar A.A. (2017) Target RNA secondary structure is a major determinant of miR159 efficacy. *Plant Physiol.,***174**, 1764-1778.

Zuo, J., Niu, Q.-W. and Chua, N.-H. (2000) An estrogen receptor-based transactivator XVE mediates highly inducible gene expression in transgenic plants. *Plant J.*, **24(2)**, 265-273.

FIGURE LEGENDS

Figure 1. Mature pollen phenotypes in wild-type and heterozygous *myb81-1* plants after DAPI-staining. (a) Normal tricellular pollen. (b-l) Abnormal pollen. (b-c) Two examples of dead pollen of different sizes. (d-f) Three examples of abnormal tricellular pollen. (g-i) Three examples of abnormal binucleate pollen. (j-l) Three examples of abnormal single nucleate pollen. Some mutant pollen grains were larger (d-l) than normal tricellular pollen, ruptured (e,h,k), or vacuolated (f,i,l). Scale bar, 10 μm.

Figure 2. Pollen development in wild type and heterozygous *myb81-1* plants. (a-s) Developing spores and pollen grains from wild type (a-h) and heterozygous mutant (i-s) plants at tetrad (a,i), free microspore (b,j), unpolarized microspore with exine accumulation (c,k), polarized microspore (d,l), early bicellular (e,m), mid-bicellular (f,n,q), late-bicellular (g,o,r), and tricellular (h,p,s) pollen stages. (t) The percentages of pollen phenotypes are shown for typical developmental stages in wild type (WT) and *myb81-1* heterozygous mutants. TET, tetrad; UMS, unpolarized microspore; PMS, polarized microspore; EBC, early bicellular pollen; LBC, late bicellular pollen; TC, tricellular pollen; AbDEG, abnormally degenerating pollen with or without residual DAPI-staining. (o,p); AbEBC, abnormal phenotype resembling early bicellular pollen (q-s); AbPMS, abnormal phenotype resembling polarized microspore (m,n). Pairs of

arrowheads (e,q,r) indicate the nascent generative cell wall formed after microspore division. Scale bar, 10μm.

Figure 3. Vacuole visualization in developing pollen of wild type (a-d, g-k) and *myb81-1* mutants (e,f,l). Developing microspores and pollen are imaged after staining with neutral red (a-f) or from transgenic plants harboring the proSCP-VHAA-mRFP1 expression cassette in wild type (a-d, g-k) and *myb81-1* heterozygous mutant (e-f, l) backgrounds. Microspores at early (g) and polarized (a, h) stages. Early (b, i) and mid-late (c,e,j,l) bicellular and tricellular (d,f,k) pollen stages. Scale bar, 10μm.

Figure 4. Expression of cell fate markers in wild type (a) and *myb81-1* mutant (b-e) pollen at anthesis. proLAT52-H2B-GFP and proMGH3-H2B-mRFP1 report vegetative cell- or germline-specific marker expression respectively. Normal tricellular pollen (a), abnormal *myb81-1* mutant pollen with one (b,c), two (d), and three (e) nuclei. Scale bar, 10μm.

Figure 5. Identification and expression analysis of *MYB81*. (a) Summary of the positional cloning of *myb81-1* and *MYB81* gene structure. The positions of molecular markers and the numbers of recombinants are shown. Eleven candidate genes are present between markers, 26940 and 27030, that contain final recombinants. The corrected *MYB81* gene structure is shown with 3 exons separated by 2 introns. (b) Complementation analysis. Percentages of normal and abnormal pollen at anthesis are shown for 6 heterozygous *myb81-1* (+/-) plants (left) and for 49 *myb81-1* (+/-) (centre) and 8 *myb81-1* (-/-) (right) mutant plants harboring the *MYB81* complementation vector. (c, d) RT-PCR analysis using 6 typical sporophytic tissues (c) and isolated developing microspores and pollen grains (d). RNA samples were prepared from seedlings (SD), roots (RT), leaves (Lf), stem (ST), young buds (YB), open flower (OF), tetrads and microspores (F2.1), microspores and early bicellular pollen (F2.2), late bicellular pollen (F2.3), tricellular pollen (F3.0) and mature pollen (MP). The histone H3.3 variant *HTR8* (At5g10980) was used as a constitutive control. The component parts of composite images were indicated by dividing lines. (e-g) Promoter-GUS analysis using transgenic lines containing proMYB81-GUS (e,g) or proMYB81-MDB-GUS (f). (h-w) Subcellular localization of MYB81 or H2B during pollen development. Isolated spores from proMYB81-MYB81-mRFP1 (h-o) or proMYB81-H2B-mRFP1 (p-w) transgenic lines were viewed at early microspore immediately after callose dissolution (h,p), early microspores with gradual accumulation of the exine (i,j,q), polarized microspore (k,r), early bicellular (l,s), mid-bicellular (m,t), late bicellular (n,u), tricellular (o,v) and mature (w) pollen stages. A pair of arrowheads marks the nascent generative cell wall formed after PMI. mn, microspore nucleus; v, vegetative nucleus; g, generative cell; s, sperm cell; vc, vacuole. Scale bar, 10μm.

Figure 6. Ectopic expression of MYB81 driven by various promoters. Mature pollen grains (a, d, e) or developing spores at tricellular (b) or bicellular (c) pollen stages are imaged from transgenic lines containing proLAT52-H2B-GFP (a), proLAT52-MYB81-GFP (b,c), or proDUO1-MYB81-mRFP1 (d,e) with (a,d,e) or without (b,c) DAPI staining. Percentages of abnormal pollen grains at mature pollen stage are shown from 15 randomly chosen proLAT52-MYB81-GFP (f) or proDUO1-MYB81-mRFP1 (g) T1 lines. Roots are viewed from transgenic plants containing proMYB81-MYB81-mRFP1 (h), proXVE-MYB81-mRFP1 in the presence of estradiol (i), or pro35S-MYB81-1-mRFP1 (j). Scale bar, 10μm.

Figure 7. MYB81 structure and phylogenetic analysis. (a) Protein structural modeling of the R2R3 domain of MYB81 in complex with DNA using SWISS-MODEL. The two-amino acids deleted from the first α-helix of the predicted mutant MYB81-1 protein are highlighted in red. (b**)** Alignment of protein sequences for Arabidopsis GAMYB family members and the mutant protein MYB81-1. The missing amino acids in MYB81-1 are boxed, red arrows indicate three tryptophan residues that form the MYB-domain hydrophobic core. (c) Phylogenetic tree of the GAMYB-like family, built with a maximum likelihood model (Tamara and Nei, 1993) and 1000 bootstraps. Two GAMYB copies in the basal angiosperm *Amborella trichopoda*, expand to form two distinct clades in *Brassicaceae*. Although most GAMYB family members possess a homolog, *Arabidopsis lyrata* (AL) has no AtMYB104 homolog and *Capsella* only has a single homolog corresponding to the AtMYB81-AtMYB104 paralogous pair. Abbreviations: *Amborella trichopoda* (AMTR), *Arabidopsis halleri* (Araha), *A. lyrata* (AL), *A. thaliana* (AtMYB), *Capsella grandiflora* (Cagra), and *C. rubella* (Carubv). * indicates incomplete sequences due to annotation errors or sequence degeneration.

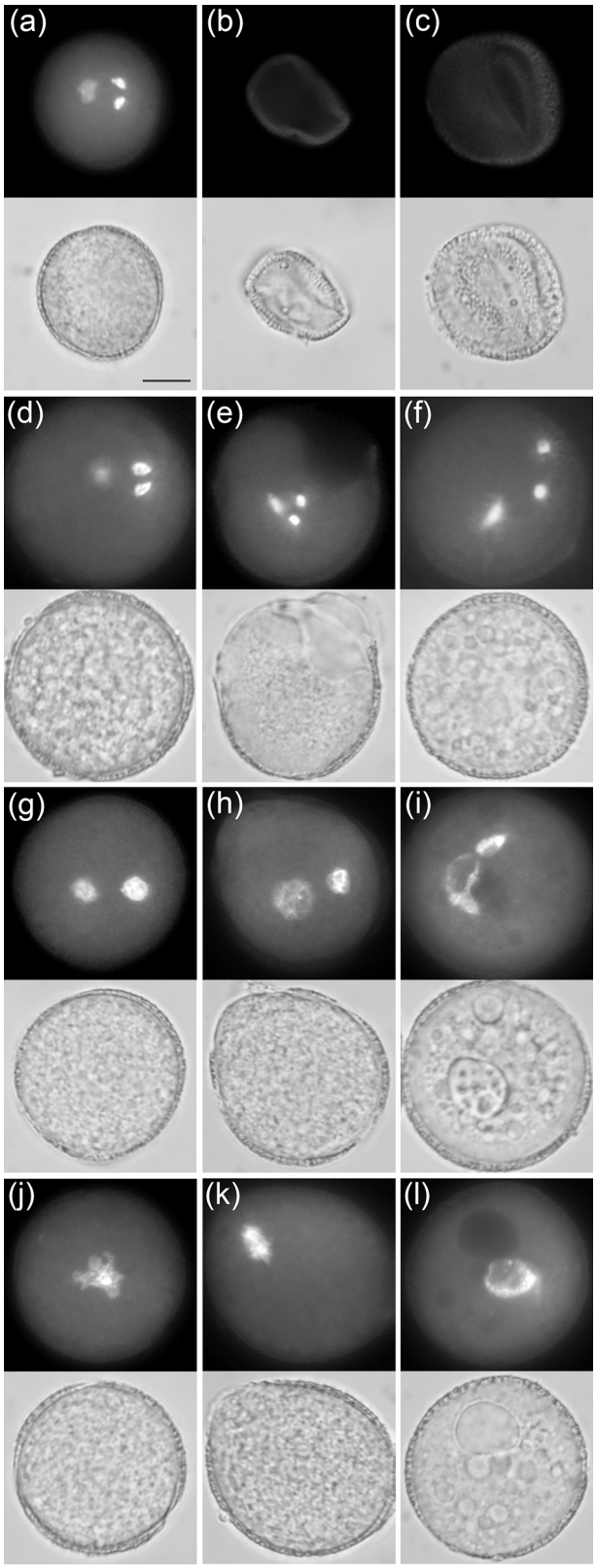

tpj_14564_f1.tif

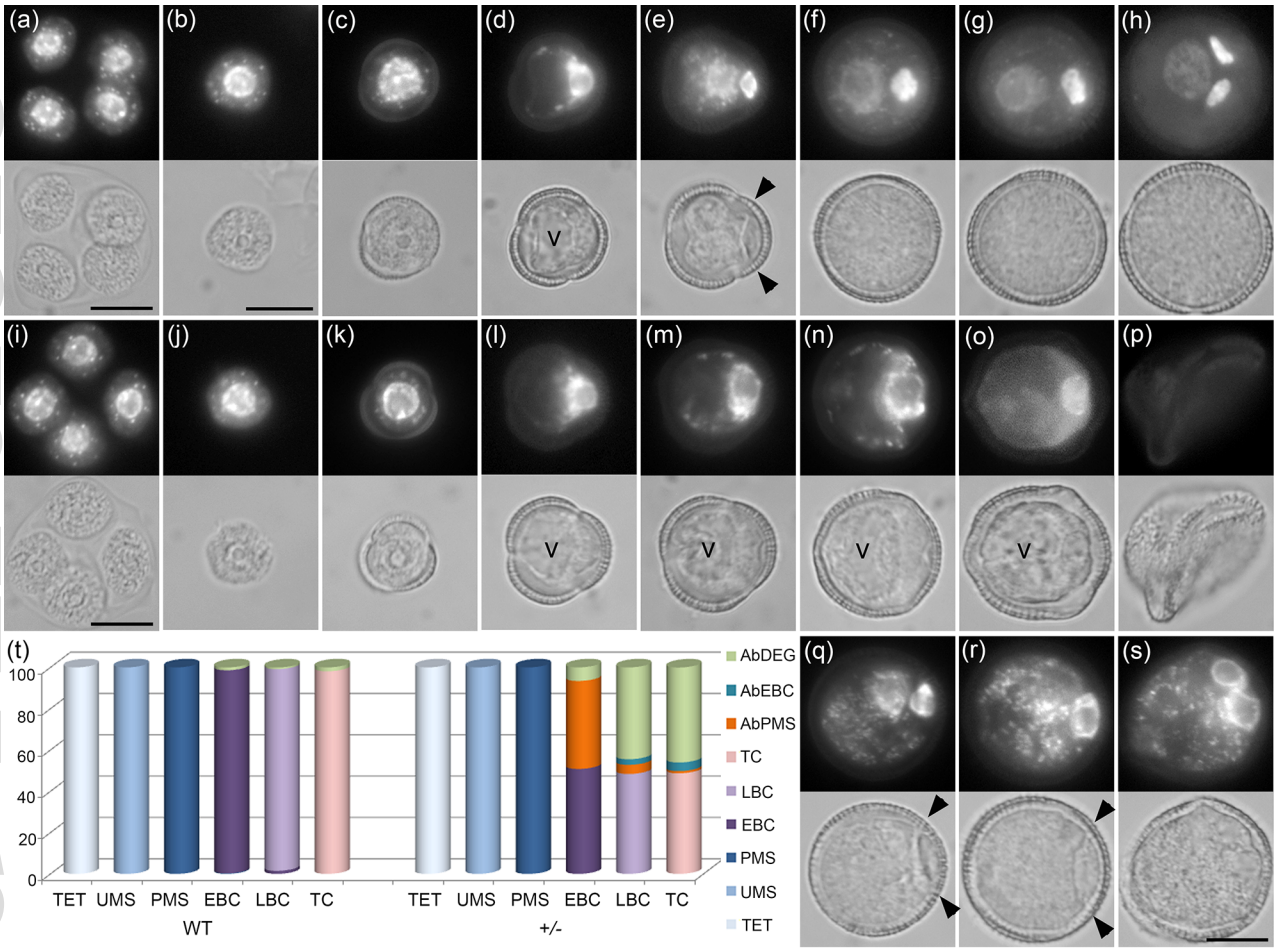

tpj_14564_f2.tif

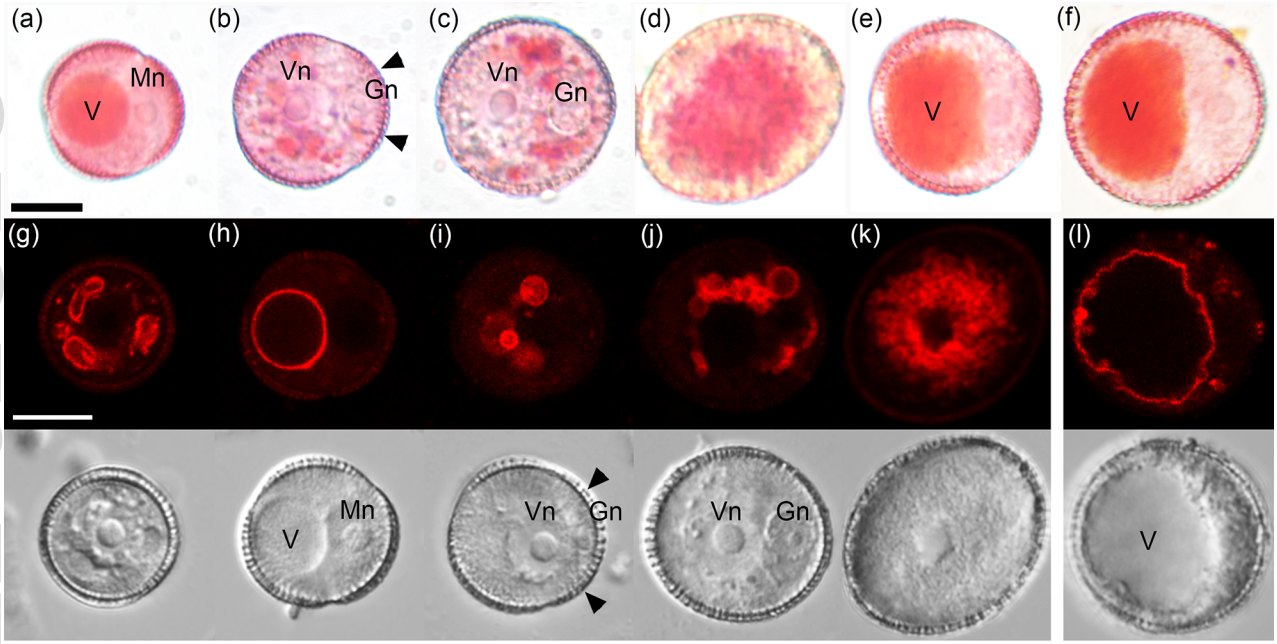

tpj_14564_f3.tif

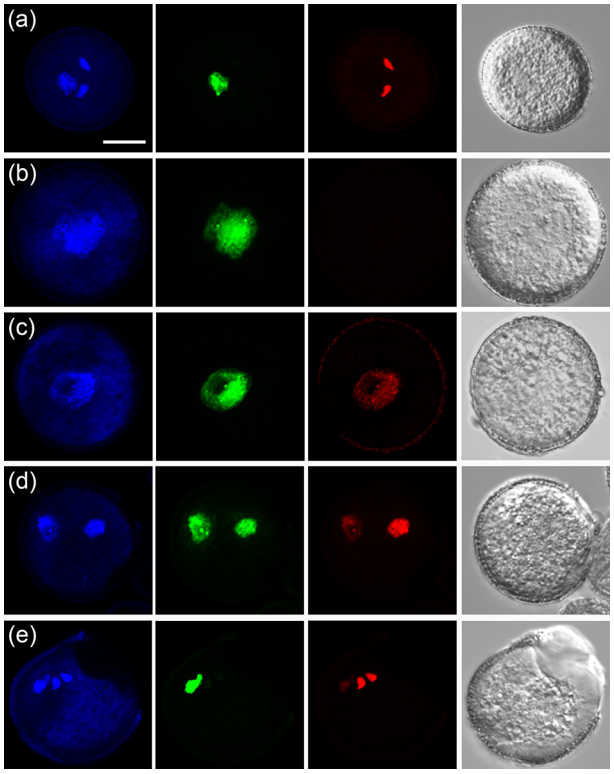

tpj_14564_f4.tif

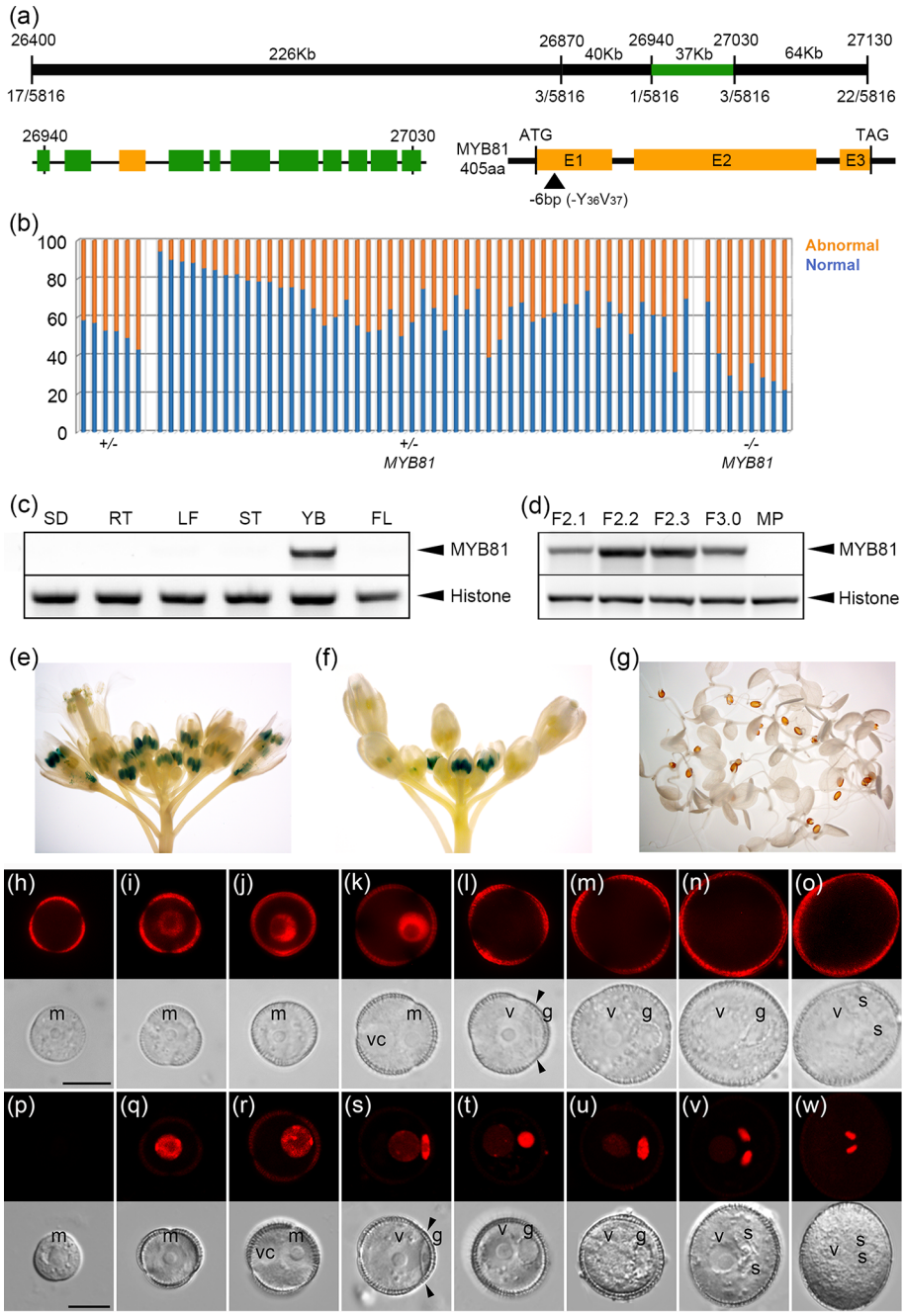

tpj_14564_f5.tif

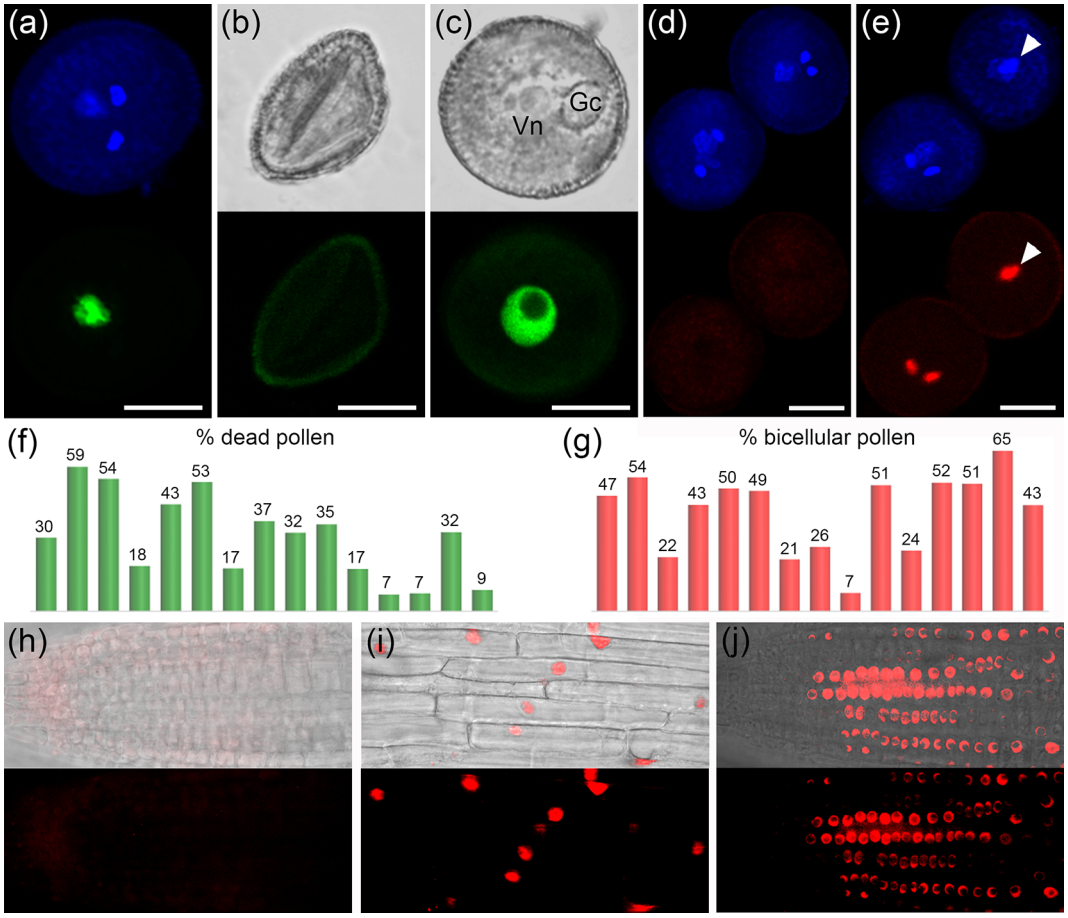

tpj_14564_f6.tif

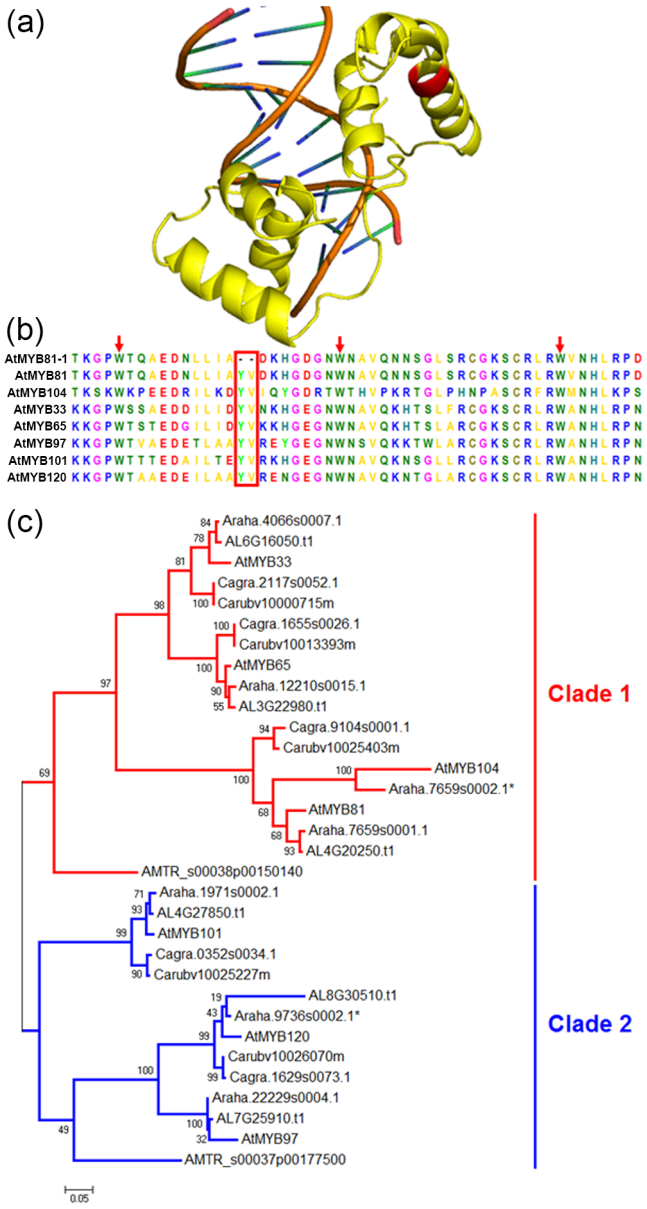

tpj_14564_f7.tif